JACS
JOURNAL OF THE AMERICAN CHEMICAL SOCIETY
pubs.acs.org/JACS
Article

Synthesis, Assembly, and Sizing of Neutral, Lanthanide Substituted Molybdenum Blue Wheels $\{Mo_{90}Ln_{10}\}$

Eduard Garrido Ribó, Nicola L. Bell, Weimin Xuan, Jiancheng Luo, De-Liang Long, Tianbo Liu, and Leroy Cronin*

Cite This: J. Am. Chem. Soc. 2020, 142, 17508−17514
Read Online
ACCESS | Metrics & More | Article Recommendations | Supporting Information

ABSTRACT: Polyoxometalate molybdenum blue (MB) complexes typically exist as discrete multianionic clusters and are composed of repeating Mo building units. MB wheels such as $\{Mo_{176}\}$ and $\{Mo_{154}\}$ are made from pentagon-centered $\{Mo_8\}$ building blocks joined by equal number of $\{Mo_1\}$ units as loin, and $\{Mo_2\}$ dimer units as skirt along the ring edge, with the ring sizes of the MB wheels modulated by the $\{Mo_2\}$ units. Herein we report a new class of contracted lanthanide-doped MB structures that have replaced all the $\{Mo_2\}$ units with lanthanide ions on the inner rim, giving the general formula $\{Mo_{90}Ln_{10}\}$. We show three examples of this new decameric $\{Mo_{90}Ln_{10}\}$ (Ln = La, Ce, and Pr) framework synthesized by high temperature reduction and demonstrate that later Ln ions result in $\{Mo_{92}Ln_9\}$ (Ln = Nd, Sm), conserving one $\{Mo_2\}$ linker unit in its structure, as a consequence of the lanthanide contraction. Remarkably the $\{Mo_{90}Ln_{10}\}$ compounds are the first examples of charge-neutral molybdate wheels as confirmed by BVS, solubility experiments, and redox titrations. We detail our full synthetic optimization for the isolation of these clusters and complete characterization by X-ray, TGA, UV−vis, and ICP studies. Finally, we show that this fine-tuned self-assembly process can be utilized to selectively enrich Ln-MB wheels for effective separation of lanthanides.

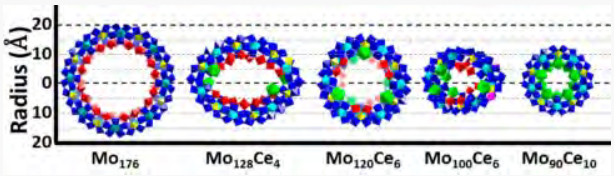

INTRODUCTION

Polyoxometalates (POMs) are a distinct class of discrete metal oxides with a wide variety of structures and properties[1,2] leading to their application in a range of scientific fields such as medicine,[3] materials science,[4] catalysis,[5] electrochemistry,[6] and magnetism.[7] Controlling the assembly of these large supramolecules, which bridge the gap between "traditional" molecular entities (<2 nm) and less precisely defined polymeric structures,[8] is a key challenge for further development of their utility. In recent years improvements in analytical and synthetic methodology have allowed the reproducible synthesis of well-defined clusters with sizes in the range of 2−6 nm with a range of topologies from Keplerate style spheres[9] to nanowheels and more complex structures such as the Mo-blue $\{Mo_{368}\}$ "lemon" shaped cluster with both positive and negative curvature.[10]

In particular, addition of heteroatoms can be used to control the ring curvature of the clusters. The unique nonavalent coordination mode of lanthanides, coupled with their oxophilicity and minimal redox behavior, has been shown to effect changes in the structure of molybdenum blue (MB) wheels.[11] These rings can be viewed as oligomeric assemblies of fundamental $\{Mo_8\}$ building blocks based on pentagonal $\{Mo(Mo)_5\}$ units[12] with $\{Mo_2\}$ and $\{Mo_1\}$ linker units, as illustrated in the archetypal tetradecameric $\{Mo_{154}\}$ (Figure 1, left). In MBs, the $\{Mo_2\}$ units (red) on the inner rim can be replaced by heterometals (Figure 1, right)[11] The incorporation of lanthanide ions in these positions acts as a "symmetry breaker" for the radial structure by adjusting the curvature and functionality of the inner surface.[11] Thus, while $\{Mo_{154}\}$ exhibits D_{7d} symmetry, increasing Ln incorporation results in a decrease in symmetry to D_3 for $\{Mo_{120}Pr_6\}$ [13] and C_2 for $\{Mo_{100}Ce_6\}$.[14]

As their name suggests, polyoxometalates clusters are traditionally anionic due to their high oxygen content and formation under reducing synthetic conditions with solvent-separated charge balancing cations.[15] Nonetheless, some low-nuclearity, formally cationic metal oxide clusters have also been reported whereby appending the cluster with highly charged metal cations yields a positive overall charge.[16] In Ln-MB structures, the introduction of the f-element reduces the negative charge in the ring since the Ln^{III} replaces the $\{Mo_2\}$ unit ($\{Mo_2O_5(H_2O)_2\}^{2+}$), with a formal 2+ charge. Müller et al. postulated a general formula that considers the basic building units of MBs to determine their charge.[17] By studying this formula in more detail, it is evident that for a case where all $\{Mo_2\}$ units would be replaced by Ln^{III} cations, the net charge

Received: July 2, 2020
Published: September 23, 2020

https://dx.doi.org/10.1021/jacs.0c07146
J. Am. Chem. Soc. 2020, 142, 17508−17514

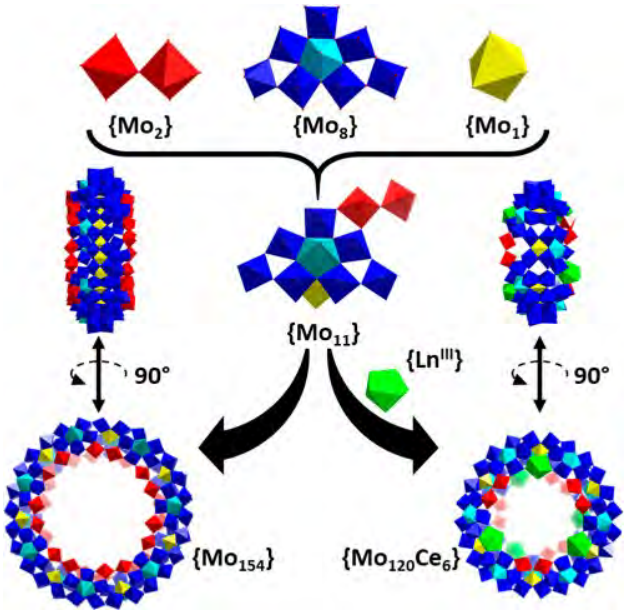

Figure 1. Schematic representation of the different MB rings obtained by adding or omitting lanthanides from the reaction mixture: $\{Mo_{154}\}$,[10b] $\{Mo_{120}Ce_6\}$.[13]

in the ring would be zero (Equation S1). Herein we detail the first synthesis of a series of formally neutral Mo blue wheels, **1**–**3**, accessed by complete replacement of the $\{Mo_2\}$ building blocks with Ln ions under reduction at elevated temperature conditions. Two intermediate compounds **4** and **5** with one $\{Mo_2\}$ building block remaining for comparison are also included herein.

In addition to "symmetry breaking" by inclusion of lanthanide ions, it can also be noted that as the number of lanthanide ions increases in a ring, the overall nuclearity of the ring decreases. This is caused by the inherent constriction caused by the replacement of the bimetallic $\{Mo_2\}$ units by a smaller monatomic Ln^{III} ion. Having these smaller building blocks interconnecting adjacent $\{Mo_8\}$ units forces them to bend in order to compensate for the shorter bridging distances, thus limiting the potential growth of the final structure (Figure 2).

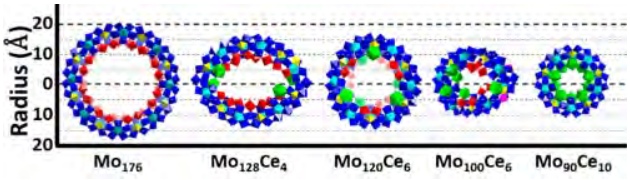

Figure 2. Schematic showing the relative change in radius (Å) of MB POMs upon increasing Ln incorporation: $\{Mo_{176}\}$,[10b] $\{Mo_{128}Ce_4\}$,[18] $\{Mo_{120}Ce_6\}$,[13] $\{Mo_{100}Ce_6\}$;[14] $\{Mo_{90}Ce_{10}\}$ this work.

Lanthanide doped MB rings can thus be classified into three categories depending on the overall number of building blocks in their main framework, tetradecameric such as $\{Mo_{150}La_2\}$,[11] dodecameric such as $\{Mo_{120}Pr_6\}$,[13] and decameric such as $\{Mo_{100}Ce_6\}$.[14] This last category represents the smallest type of MB rings known, and we believe it may be impossible to access a LnMB ring that has less than 10 $\{Mo_8\}$ building blocks in its backbone. This is because each of the monomeric building block units changes very little between the different oligomers. As the number of monomers decreases, the ring contracts, reaching at least 7.9 Å in the decamer (this work). Our models suggest that the equivalent octamer would require a 3.3 Å diameter cavity which is likely too small a space for the 8 endo-oxo ligands to coexist (see Supporting Information Figure S2). For this reason we believe that the $\{Mo_{90}Ln_{10}\}$ framework presented herein is not only the first formally charge neutral polyoxometalate but also the smallest accessible molybdenum blue wheel of this type. Here we detail the synthesis of clusters **1**–**5**, a study of their structural properties, and their use for the selective enrichment of lanthanide ions.

RESULTS AND DISCUSSION

Synthesis of 1–5. The formally neutral framework $\{Mo_{90}Ln_{10}\}$ (Ln = Ce **1**, La **2**, Pr **3**, Figure 3a and Figure 3b) was synthesized from a one-pot reaction of an acidified aqueous mixture of $Na_2MoO_4{\cdot}2H_2O$ (0.2 mmol), $[N_2H_4]{\cdot}2HCl$ (0.01 mmol), and $LnCl_3{\cdot}7H_2O$ (0.05 mmol) heated in a capped, needle-punctured vial at 100 °C. The combined reagents changed from a colorless mixture to transparent, dark blue solution before heating. The key variables for the formation of $\{Mo_{90}Ln_{10}\}$ were found to be both accurate pH tuning and constant high temperatures. MB rings (e.g., $\{Mo_{154}\}$) are commonly synthesized under acidic conditions at around pH 1.0; however, by slight raising of the pH value close to 2, the $\{Mo_2\}$ units become less stabilized and more prone to substitution by Ln^{III} ions. Yet a balance needs to be found since increasing the pH to higher values than 2.2 resulted in the oxidation of the Mo^V centers, while lower pH yielded only amorphous precipitate (Table S1). Previously reported Ln-MBs have been synthesized from reactions heated to between 20 and 90 °C. By heating the sample to 100 °C, we bring the system to the boundary of hydrothermal and standard reaction conditions, switching from kinetic to

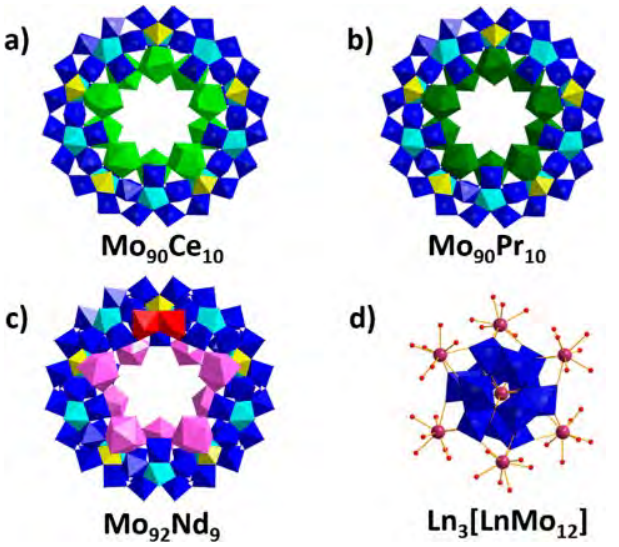

Figure 3. Polyhedral view of the solid state structure of **1** (a), **3** (b), and **4** (c). The general structure obtained as an oxidation product $Ln_3[LnMo_{12}]$, where Ln = La, Ce, Pr, Nd is shown in (d). {Mo1}: yellow polyhedra. {Mo8}: blue polyhedra with central pentagonal units in cyan polyhedra. Nd: pink polyhedra. Ce: green polyhedra. Pr: dark green polyhedra. Ln ion: purple ball. O: red ball.

https://dx.doi.org/10.1021/jacs.0c07146
J. Am. Chem. Soc. 2020, 142, 17508–17514

thermodynamic control. This is key to complete replacement of the $\{Mo_2\}$ units due to the fact that lanthanide ions are intrinsically smaller building blocks than $\{Mo_2\}$; therefore each replacement results in additional constriction of the ring.

Figure 4 highlights the respective distances between corresponding $\{Mo_8\}$ polyhedra corners across the $\{Mo_2\}$/

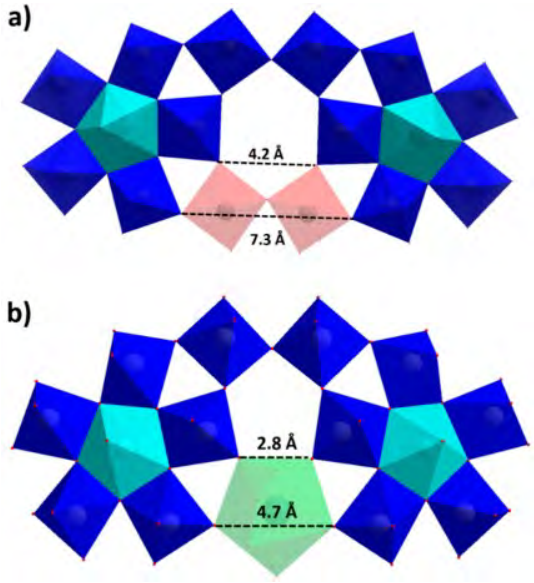

Figure 4. Comparison of the distances between equivalent oxygen atoms for two adjacent $\{Mo_8\}$ units for Mo_{154} (a) and $Mo_{90}Ln_{10}$ (b).

Ln binding sites for the parent $\{Mo_{154}\}$ (a) and the $\{Mo_{90}Ln_{10}\}$ (b) rings. It can be observed how the overall distances between equivalent oxygen atoms pairs are reduced nearly by half (from 7.3 to 4.7 Å for the inner rim and from 4.2 to 2.8 Å for the belt polyhedra). This constriction created between building units causes the increase in ring curvature and thus the structure to lose some of its $\{Mo_8\}$ building blocks changing from a tetradecameric ring in the case of the $\{Mo_{154}\}$ to a decameric ring for the $\{Mo_{90}Ln_{10}\}$. By heating the reaction mixture to temperatures lower than 100 °C for a short period of time (e.g., 3 h), the less constrained $\{Mo_{120}Ln_6\}$ [13] or $\{Mo_{130}Ln_6\}$ [19] are isolated (Figure 5), suggesting these may be kinetic intermediates in the synthesis of $\{Mo_{90}Ln_{10}\}$. The prolonged exposure to high temperatures provides the required energy to overcome the constriction of replacing all the $\{Mo_2\}$ units from the parent ring required for the formation of the small neutral rings, **1**−**3**.

The lanthanide contraction results in smaller ionic radii as we cross the 4f period which becomes a key factor in the replacement of $\{Mo_2\}$ from Nd onward.[20] Utilizing $NdCl_3 \cdot 6H_2O$ or $SmCl_3 \cdot 6H_2O$ under the same conditions as for **1**−**3** did not result in the formation of $\{Mo_{90}Ln_{10}\}$ but rather $\{Mo_{92}Ln_9\}$, (Ln = Nd **4**, Sm **5**, Figure 3c). This suggests there may be a limit to the ability of the decameric wheel to contract; thus $\{Mo_{90}Pr_{10}\}$ represents the smallest possible neutral MB.

With later lanthanides (Eu, Gd, Tb, Dy, Ho, Er, Yb) only the Silverton-like cluster, $Ln_3[LnMo_{12}]$, is observed under these conditions (Figure 3d). This cluster is an isostructure of $Gd_3[GdMo_{12}]$,[21] which appears as yellow cubic crystals in the case of Ce and as colorless crystals for the other lanthanides. This cluster is also observed upon extended heating of complexes **1**−**5** under non-reducing conditions (i.e., after

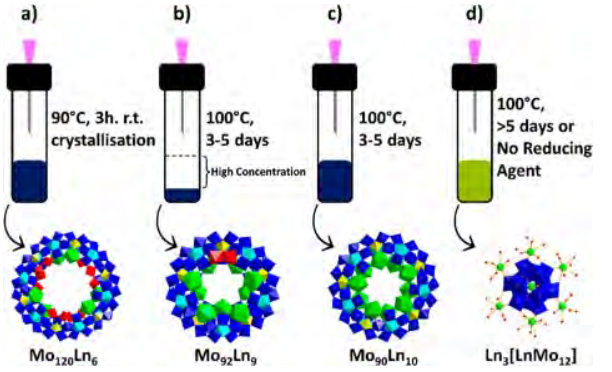

Figure 5. Schematic representation of the different compounds obtained under different conditions. The same acidified molybdate solution can yield these different clusters if they (a) crystallize at room temperature, (b) are under reducing conditions with high evaporation rate, (c) are under reducing conditions, or (d) are under nonreducing hydrothermal conditions.

consumption of reducing agent). This means that there is a structural transformation from the $\{Mo_{90}Ln_{10}\}$ framework to the smaller $Ln_3[LnMo_{12}]$ that will be later discussed.

The Important Choice of Lanthanide Salts. In MB syntheses, it has been proven that modifying the counterions associated with the starting materials can yield different self-assembled products; however this has previously mostly been demonstrated by modifying the molybdenum source, the acid, or the reducing agent used.[22] The main focus of POM synthesis tends to be directed toward tuning the reaction conditions rather than modifying these starting materials. Since there were examples in the literature where nitrate salts were used as the Ln source, we did not hesitate in using them for the synthesis of **3** and **4**. However, the outcome of these reactions differed greatly from those of compounds **1** and **2** since, despite using the same reaction conditions, **1** and **2** were obtained as dark blue crystals in a dark blue solution while **3** and **4** were never observed. Instead, the solution turned pale yellow and transparent crystals of $Ln_3[Mo_{12}Ln]$ appeared. After exhaustion of other possibilities, changing the lanthanide source from nitrates to chlorides allowed us to obtain compounds **3** and **4**. It would seem that despite having a similar field strength, these two ligands are not interchangeable when exposed to high temperatures.

Determination of the Formulas of 1−5. The determination of the formulas of the Mo-blues has been well established and requires a series of analytical techniques including redox titrations, UV−vis−NIR spectroscopy, bond valence sum analysis (BVS), elemental analysis and thermogravimetric analysis (TGA), in addition to single-crystal X-ray diffraction analysis (see Supporting Information for details).[17] Here **1** was selected to exemplify the general approach used to determine the formula. First, BVS calculations were carried out on all the Mo and O centers, revealing that **1** is composed of a 20-electron reduced anionic ring containing 10 singly protonated oxygen atoms.[23] Although these 20 electrons are delocalized over all Mo centers, BVS indicates that the Mo centers on $\{Mo_8\}$ are more likely to be Mo^{VI} and reduced Mo^{V} centers are near the backbone of the ring, consistent with previous work.[18] The 10 equivalent oxo atoms are singly protonated and are situated in the equatorial plane, linking two neighboring $\{Mo_8\}$ units as well as $\{Mo_1\}$ units. Meanwhile, redox titration confirmed the overall reduction state for **1**, and

https://dx.doi.org/10.1021/jacs.0c07146
J. Am. Chem. Soc. 2020, 142, 17508−17514

UV−vis−NIR spectroscopy showed the characteristic absorption band of MB which is centered at around 745 nm. Additionally, elemental analysis confirms the framework of **1** consists of 90 Mo and 10 Ce atoms, consistent with the structural refinement done using the single-crystal X-ray diffraction data. Taking into consideration the information obtained from the calculations above, along with elemental analysis, it is possible to determine the overall building-block scheme and overall charge for **1** as $[\{Mo_1\}_{10}\{Mo_8\}_{10}\{Ce(H_2O)_5\}_{10}] \equiv [\{Mo_8^{V/VI}O_{27}(OH)(H_2O)_3Mo^{VI/V}\}_{10}\{Ce^{III}(H_2O)_5\}_{10}]$.[24] Finally, the TGA curve of **1** exhibits a total weight loss of 16.5% from rt to 150 °C, which corresponds to ∼180 guest water molecules. On the basis of the discussion above, the formula of **1** could therefore be determined as $\{Mo_{90}Ce_{10}O_{280}(H_2O)_{80}H_{10}\}\cdot 180H_2O$. The formulas of compounds **2**−**5** are determined in a similar manner. Compounds **1**−**5** could be formulated as follows:

1, $\{Mo_{90}Ce_{10}O_{280}(H_2O)_{80}H_{10}\}\cdot 180H_2O$
2, $\{Mo_{90}La_{10}O_{280}(H_2O)_{80}H_{10}\}\cdot 191H_2O$
3, $\{Mo_{90}Pr_{10}O_{280}(H_2O)_{80}H_{10}\}\cdot 188H_2O$
4, $H\{Mo_{92}Nd_9O_{285}(H_2O)_{77}H_{10}\}\cdot 185H_2O$
5, $H\{Mo_{92}Sm_9O_{285}(H_2O)_{77}H_{10}\}\cdot 180H_2O$

Solution Studies. It is known that metal oxide-based molecular clusters bear multiple metal cations (Lewis acid sites) with influential coordinated water ligands. These nanosize clusters are intermediate in size between simple ions and colloids[25] and have a distinctive solution behavior when charged (macroions) in aqueous solution: they tend to spontaneously assemble into stable, uniform, hollow spherical "blackberry" structures instead of existing as discrete ions in dilute solution.[26] The formation of these structures is driven by counterion-mediated electrostatic attractions and hydrogen bonding, as opposed to van der Waals forces, hydrophobic interactions, or chemical reactions.[25]

The rings are neutral in solid state; however, they are found to be negatively charged upon dissolving in water. Encapsulation experiments reveal that the $\{Mo_{90}Ce_{10}\}$ ring binds strongly with positively charged cetrimonium bromide (CTAB) surfactant (Figure S21), demonstrating the negative charge of the wheel arising from the deprotonation of coordinated water ligands. From TGA studies, the number of CTAB absorbed on the surface of $\{Mo_{90}Ce_{10}\}$ increases at higher pH values (Figures S22−S27), indicating more deprotonated water ligands in less acidic environment. This is consistent with the general trend of deprotonation of water ligands in response to solution pH, similar to a weak acid.[27]

For the self-assembly study, 0.05 mg mL^{-1} $\{Mo_{90}Ce_{10}\}$ solution at pH 1 was used and strong divalent cation Ba^{2+} was added to enhance the macroion−counterion attraction. As monitored by static light scattering (SLS), the scattered intensity of $\{Mo_{90}Ce_{10}\}$ solution exhibits a sigmoidal-type self-assembly process (Figure S28), very similar to the previously reported kinetics of blackberry structure formation.[28] At equilibrium, the hydrodynamic radius (R_h) measured from dynamic light scattering (DLS) is angle independent, suggesting the spherical assemblies in solution (Figure 6a). With the addition of more Ba^{2+} ions, the assembly size becomes larger (Figure S29), which confirms that the self-assembly is a charge-regulated process. Combined with the radius of gyration (R_g) obtained from SLS experiments (Figure S30), the R_g/R_h ratio is 0.95, close to the theoretic value for a hollow sphere.[29] Furthermore, TEM images show membrane-like structures with uniform electron density after the collapse of hollow spheres (Figure 6b).

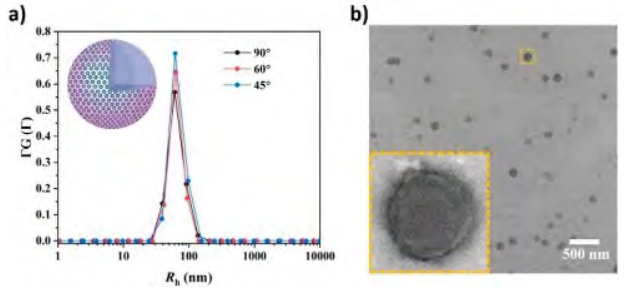

Figure 6. (a) DLS results of a solution of **1**, $\{Mo_{90}Ce_{10}\}$ (40 equiv of $BaCl_2$) at different scattering angles. The R_h value is 62(±5) nm. (b) TEM images obtained from $\{Mo_{90}Ce_{10}\}$ solution with 40 equiv of $BaCl_2$.

Crystal Structures of 1−5. Single-crystal X-ray structural analysis reveals that compounds **1**−**3** are isostructural; therefore for brevity we will only discuss compound **1** in detail. **1** crystallizes in the orthorhombic system with the space group *Pccn* and features a nanoring $\{Mo_{90}Ce_{10}\}$, composed of 10 $\{Mo_8\}$ units, 10 $\{Mo_1\}$ units, 10 $\{Ce^{III}(H_2O)_5\}$ units, and no $\{Mo_2\}$ units since all have been replaced (Figure 3a). The 10 Ce^{3+} ions are distributed symmetrically on both the upper and lower rims of $\{Mo_{90}Ce_{10}\}$, making the whole wheel exhibit a D_{5d} symmetry. This is lower than the D_{7d} symmetry of the $\{Mo_{154}\}$ but higher than other Ln-MBs due to the complete replacement of the $\{Mo_2\}$ moiety. Thus, the wheel displays a rather high symmetry structure with an outer and inner ring diameter of about 26 and 7 Å, respectively, at its most elongated points, significantly smaller than the 36 and 20 Å for the $\{Mo_{154}\}$.

Compounds **4** and **5** crystallize in the orthorhombic system with *Cmca* space group and consist of 10 $\{Mo_8\}$ units, 10 $\{Mo_1\}$ units, 1 $\{Mo_2\}$ unit, and 9 $\{Nd(H_2O)_5\}$ in the case of **4** and 9 $\{Sm(H_2O)_5\}$ for **5**. They differ from compounds **1**−**3** in the fact that one of the original 10 $\{Mo_2\}$ units is not replaced by a Ln^{III} ion but instead remains in the structure. This $\{Mo_2'\}$ unit is edge sharing (i.e., κ^2) instead of the corner sharing mode (κ^1) which is normally observed in MBs such as $\{Mo_{154}\}$. The difference between these mid-series ions and the early f-block metals appears to be due to the lanthanide contraction, since Nd and Sm have slightly smaller ionic radii than those where the $\{Mo_{90}Ln_{10}\}$ framework has been successfully obtained.[20] We hypothesize that the constriction of a wheel containing 10 Nd ions would be too great and would destabilize the structure; thus a single $\{Mo_2'\}$ unit remains in the structure to alleviate this pressure. However, we also obtained the $\{Mo_{92}Ln_9\}$ structure with La, Ce, and Pr during syntheses where the reaction vial was not completely sealed, meaning the solvent evaporated more than usual. These isostructures demonstrated that it was possible to obtain $\{Mo_{92}Ln_9\}$ for the series from La to Sm while the smaller $\{Mo_{90}Ln_{10}\}$ was only achievable with the larger subset La to Pr. This suggests that $\{Mo_{92}Ln_9\}$ is in fact an intermediate of the reaction that can be isolated if the reaction cannot be completed, be it because of too much impediment from the ring constriction or because of solution saturation (Figure 7).

Magnetic Studies. Lanthanide ions are highly sought after for their unique magnetic properties, and many single molecule magnets (SMMs) utilize lanthanide ions.[30] With 10

https://dx.doi.org/10.1021/jacs.0c07146
J. Am. Chem. Soc. 2020, 142, 17508−17514

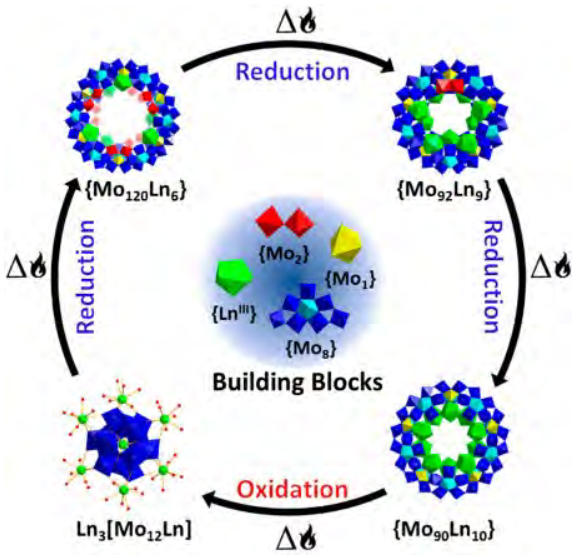

Figure 7. Structure transformation from $\{Mo_{120}Ln_6\}$ to $\{Mo_{92}Ln_9\}$ to $\{Mo_{90}Ln_{10}\}$ and finally to $Ln_3[LnMo_{12}]$ depending on the reaction conditions.

lanthanides per molecule in close proximity we sought to understand the magnetic behavior of our wheels. For all the compounds antiferromagnetic coupling was observed. This can be rationalized by the highly symmetric structure of the cluster allowing for each spin to be canceled out and no clear axis of magnetization to emerge.

Lanthanide Separation. Most rare earths occur in nature as ores that contain several lanthanides, and the similarity in their chemistry and ionic radii has made selective isolation of the 14 4f ions challenging, particularly the separation of ions from their nearest neighbors, e.g., Nd/Sm.[31] A range of techniques including ion-exchange chromatography,[32] and solvent extraction[33] have been utilized to isolate pure Ln(III) salts. Recently it was shown that self-assembly processes could be used to selectively enrich Ln ions in inorganic materials based solely on ionic radius.[34] Considering how minor differences in the Ln(III) ionic radius can strongly affect the self-assembly of these clusters, we investigated whether it would be possible to achieve selective enrichment of Ln ions from binary mixtures in solution by self-assembly alone.

Initial attempts using 0.5 equiv of each La and Eu were poorly yielding, producing too little material for accurate analysis. However, using 1 equiv of each Ln ion allowed for the isolation of dark blue crystals along with a light blue amorphous precipitate and blue solution, each of which was analyzed by ICP-OES (detailed synthesis can be found in the Supporting Information). The results showed a higher content of La compared to Eu (2.72:1), comfirming our expectations that uptake of the larger lanthanide is favored in these reactions. Concordantly, the mother liquor contained a lower ratio of La:Eu (0.85:1). Table 1 shows the separation factors for all binary mixtures investigated in this study. The separation factors (SF) show a positive correlation with the difference in ionic radius (Δr) between the ions, with La/Er showing the highest separation factor observed thus far. These results support our hypothesis that the formation of the $\{Mo_{90}Ln_{10}\}$ cluster is determined by lanthanide ionic radius with smaller ions unable to form this cluster and thus forming smaller molybdates such as the Silverton $Ln_3[Mn_{12}Ln]$ cluster

Table 1. Selective Enrichment of Larger Lanthanide Ions from Binary Mixtures

lanthanide mix	Δr (pm)	separation factor
La/Sm	8.16	2.08
La/Eu	9.36	3.19
La/Er	15.20	15.30
Pr/Sm	4.70	1.88
Pr/Eu	5.90	2.67
Pr/Er	11.70	7.20
Nd/Sm	3.10	1.58
Nd/Eu	4.30	2.41

and remaining in solution. Importantly, our results show selective enrichment of "nearest neighbor" lanthanides which are known to be particularly challenging to separate.

CONCLUSIONS AND FUTURE WORK

We have successfully synthesized the first example of a neutral molybdenum blue ring by developing a new synthetic strategy using lanthanide ions (La, Ce, Pr) that replace all the $\{Mo_2\}$ building blocks. High temperatures, pH control, and carefully choosing the starting reagents are essential for a successful synthesis. All three structures share the same framework of $\{Mo_{90}Ln_{10}\}$ with the lanthanides occupying the inner circle of the ring. These structures are the first example of a neutral MB wheel and the smallest ones reported to date. In concordance with previous literature, we hypothesize this framework to be the smallest possible in a MB ring. A similar structure has been obtained for Nd and Sm where one of the $\{Mo_2\}$ units remains in the cluster due to the inherent constriction caused by the smaller ionic radius of these lanthanides. These structures are thought to be a reaction intermediate since it was also observed with larger lanthanide ions in some reactions. Continued exposure to these high temperatures eventually consumes all the reducing agent present in the system, causing a structure transformation from $\{Mo_{90}Ln_{10}\}$ to $Ln_3[LnMo_{12}]$, which in turn can be rereduced to the $\{Mo_{120}Ln_6\}$ and, if heated again, back to the $\{Mo_{90}Ln_{10}\}$.

As the ionic radius of the lanthanide plays a role in the structure formation, several tests of lathanide separation were conducted showing promising results separating early lanthanides from later ones. Taking advantage of the subtleties of the self-assembly process, we have demonstrated effective enrichment of lanthanide ions from binary mixtures in the synthesis of $\{Mo_{90}Ln_{10}\}$. In future we will build upon these results to utilize the self-assembly of molybdenum blue POMs for high-yielding scalable lanthanide separation processes.

ASSOCIATED CONTENT

Supporting Information

The Supporting Information is available free of charge at https://pubs.acs.org/doi/10.1021/jacs.0c07146.

Detailed synthetic procedures, crystallography, TGA, BVS calculations, and IR and UV−vis results (PDF)

Data for $\{Mo_{90}Ce_{10}O_{280}(H_2O)_{80}H_{10}\}\cdot 180H_2O$ (**1**) (CIF)

Data for $\{Mo_{90}La_{10}O_{280}(H_2O)_{80}H_{10}\}\cdot 191H_2O$ (**2**) (CIF)

Data for $\{Mo_{90}Pr_{10}O_{280}(H_2O)_{80}H_{10}\}\cdot 188H_2O$ (**3**) (CIF)

Data for $H\{Mo_{92}Nd_9O_{285}(H_2O)_{77}H_{10}\}\cdot 185H_2O$ (**4**) (CIF)

https://dx.doi.org/10.1021/jacs.0c07146
J. Am. Chem. Soc. 2020, 142, 17508−17514

Data for $H\{Mo_{92}Sm_9O_{285}(H_2O)_{77}H_{10}\}\cdot 180H_2O$ (5) (CIF)

AUTHOR INFORMATION

Corresponding Author

Leroy Cronin − *School of Chemistry, University of Glasgow, Glasgow G12 8QQ, United Kingdom;* orcid.org/0000-0001-8035-5757; Email: Lee.Cronin@Glasgow.ac.uk

Authors

Eduard Garrido Ribó − *School of Chemistry, University of Glasgow, Glasgow G12 8QQ, United Kingdom;* orcid.org/0000-0002-5837-5185

Nicola L. Bell − *School of Chemistry, University of Glasgow, Glasgow G12 8QQ, United Kingdom;* orcid.org/0000-0002-7497-9667

Weimin Xuan − *School of Chemistry, University of Glasgow, Glasgow G12 8QQ, United Kingdom;* orcid.org/0000-0003-0288-1633

Jiancheng Luo − *Department of Polymer Science, The University of Akron, Akron, Ohio 44325, United States;* orcid.org/0000-0002-3766-4922

De-Liang Long − *School of Chemistry, University of Glasgow, Glasgow G12 8QQ, United Kingdom;* orcid.org/0000-0003-3241-2379

Tianbo Liu − *Department of Polymer Science, The University of Akron, Akron, Ohio 44325, United States;* orcid.org/0000-0002-8181-1790

Complete contact information is available at: https://pubs.acs.org/10.1021/jacs.0c07146

Notes

The authors declare no competing financial interest.

ACKNOWLEDGMENTS

This work was supported by LCs EPSRC grants (Grants EP/J015156/1; EP/L023652/1; EP/I033459/1; EP/J015156/1; EP/K023004/1; EP/L023652/1) and the ERC Advanced Grant (ERC-ADG, 670467 SMART-POM). T.L. acknowledges support by NSF (Grant CHE1904397) and the University of Akron. The authors thank Prof. Mark Murrie and Emma Regincós Martí for assistance with the SQUID measurements as well as for the helpful discussions on the magnetic properties of the reported comounds. We thank Diamond Light Source for time on Beamline I19 under Proposal CY22214.

REFERENCES

(1) Miras, H. N.; Mathis, C.; Xuan, W.; Long, D.-L.; Pow, R.; Cronin, L. Spontaneous formation of autocatalytic sets with self-replicating inorganic metal oxide clusters. *Proc. Natl. Acad. Sci. U. S. A.* **2020**, *117*, 10699−10705.

(2) (a) Long, D.-L.; Burkholder, E.; Cronin, L. Polyoxometalate Clusters, Nanostructures and Materials: From Self Assembly to Designer Materials and Devices. *Chem. Soc. Rev.* **2007**, *36*, 105−121. (b) Long, D.-L.; Tsunashima, R.; Cronin, L. Polyoxometalates: Building Blocks for Functional Nanoscale Systems. *Angew. Chem., Int. Ed.* **2010**, *49*, 1736−1758.

(3) Hasenknopf, B. Polyoxometalates: introduction to a class of inorganic compounds and their biomedical applications. *Front. Biosci., Landmark Ed.* **2005**, *10*, 275−287.

(4) Coronado, E.; Gomez-Garcia, C. J. Polyoxometalate-Based Molecular Materials. *Chem. Rev.* **1998**, *98*, 273−296.

(5) (a) Hill, C. L. Polyoxometalates in Catalysis. *J. Mol. Catal. A: Chem.* **2007**, *262*, 2−6. (b) Zhou, Y.; Guo, Z.; Hou, W.; Wang, Q.; Wang, J. Polyoxometalate-based phase transfer catalysis for liquid-solid organic reactions: a review. *Catal. Sci. Technol.* **2015**, *5*, 4324−4335.

(6) Sadakane, M.; Steckhan, E. Electrochemical Properties of Polyoxometalates as Electrocatalysts. *Chem. Rev.* **1998**, *98*, 219−238.

(7) Müller, A.; Kogerler, P.; Dress, A. W. M. Giant metal-oxide-based spheres and their topology: from pentagonal building blocks to keplerates and unusual spin systems. *Coord. Chem. Rev.* **2001**, *222*, 193−218.

(8) Müller, A.; Gouzerh, P. From linking of metal-oxide building blocks in a dynamic library to giant clusters with unique properties and towards adaptative chemistry. *Chem. Soc. Rev.* **2012**, *41*, 7431−7463.

(9) Müller, A.; Krickemeyer, E.; Bögge, H.; Schmidtmann, M.; Peters, F. Organizational Forms of Matter: An Inorganic Super Fullerene and Keplerate Based on Molybdenum Oxide. *Angew. Chem., Int. Ed.* **1998**, *37*, 3359.

(10) (a) De La Oliva, A. R.; Sans, V.; Miras, H. N.; Yan, J.; Zang, H.-Y.; Richmond, C. J.; Long, D.-L.; Cronin, L. Assembly of a Gigantic Polyoxometalate Cluster $\{W_{200}Co_8O_{660}\}$ in a Networked Reactor System. *Angew. Chem., Int. Ed.* **2012**, *51*, 12759−12762. (b) Müller, A.; Gouzerh, P. From linking of metal-oxide building blocks in a dynamic library to giant clusters with unique properties and towards adaptive chemistry. *Chem. Soc. Rev.* **2012**, *41*, 7431−7463.

(11) (a) Yamase, T.; Ishikawa, E.; Abe, Y.; Yano, Y. Photoinduced self-assembly to lanthanide-containing molybdenum-blue super-clusters and molecular design. *J. Alloys Compd.* **2006**, *408*−*412*, 693−700. (b) Ma, X.; Yang, W.; Chen, L.; Zhao, J. Significant developments in rare-earth-containing polyoxometalate chemistry: synthetic strategies, structural diversities and correlative properties. *CrystEngComm* **2015**, *17*, 8175−8197.

(12) Müller, A.; Serain, C. Soluble Molybdenum Blues - "des Pudels Kern". *Acc. Chem. Res.* **2000**, *33*, 2−10.

(13) Müller, A.; Beugholt, C.; Bögge, H.; Schmidtmann, M. Influencing the Size of Giant Rings by Manipulating their Curvatures: $Na_6[Mo_{120}O_{366}(H_2O)_{48}H_{12}\{Pr(H_2O)_5\}_6]\cdot(\sim 200H_2O)$ with Open Shell Metal Centers at the Cluster Surface. *Inorg. Chem.* **2000**, *39*, 3112−3113.

(14) Xuan, W.; Surman, A. J.; Miras, H. N.; Long, D.; Cronin, L. Controlling the Ring Curvaure, Solution Assembly, and Reactivity of Gigantic Molybdenum Blue Wheels. *J. Am. Chem. Soc.* **2014**, *136*, 14114−14120.

(15) Müller, A.; Roy, S. En route from the mystery of molybdenum blue via related manipulatable building blocks to aspects of materials science. *Coord. Chem. Rev.* **2003**, *245*, 153−166.

(16) Points, L. J.; Cooper, G. J. T.; Dolbecq, A.; Mialane, P.; Cronin, L. An all-inorganic polyoxometalate-polyoxocation chemical garden. *Chem. Commun.* **2016**, *52*, 1911−1914.

(17) Müller, A.; Krickemeyer, E.; Bögge, H.; Schmidtmann, M.; Beugholt, C.; Das, S. K.; Peters, F. Giant Ring-Shaped Building Blocks Linked to Form a Layered Cluster Network with Nanosized Channels: $[Mo^{VI}_{124}Mo^{V}_{28}O_{429}(\mu_3\text{-}O)_{28}H_{14}(H_2O)_{66.5}]^{16-}$. *Chem. - Eur. J.* **1999**, *5*, 1496−1502.

(18) Cronin, L.; Beugholt, C.; Krickemeyer, E.; Schmidtmann, M.; Bögge, H.; Kögerler, P.; Luong, T. K. K.; Müller, A. "Molecular symmetry breakers" generating metal-oxide-based nanoobject fragments as synthons for complex structures: $[\{Mo_{128}Eu_4O_{388}H_{10}(H_2O)_{81}\}\}_2]^{20-}$, a giant-cluster dimer. *Angew. Chem., Int. Ed.* **2002**, *41*, 2805−2808.

(19) Xuan, W.; Pow, R.; Long, D.; Cronin, L. Exploring the Molecular Growth of Two Gigantic Half-Closed Polyoxometalate Clusters $\{Mo_{180}\}$ and $\{Mo_{130}Ce_6\}$. *Angew. Chem., Int. Ed.* **2017**, *56*, 9727−9731.

(20) Quadrelli, E. A. Lanthanide Contraction over the 4f Series Follows a Quadratic Decay. *Inorg. Chem.* **2002**, *41*, 167−169.

(21) Wu, C.; Lu, C.; Zhuang, H.; Huang, J. Hydrothermal Assembly of a Novel Three-Dimensional Framework Formed by $[GdMo_{12}O_{42}]^{9-}$

Anions and Nine Coordinated Gd^{III} Cations. *J. Am. Chem. Soc.* **2002**, *124*, 3836−3837.
(22) Xuan, W.; Pow, R.; Watfa, N.; Zheng, Q.; Surman, A. J.; Long, D.; Cronin, L. Stereoselective Assembly of Gigantic Chiral Molybdenum Blue Wheels Using Lanthanide ions and Amino Acids. *J. Am. Chem. Soc.* **2019**, *141*, 1242−1250.
(23) Brown, I. D. In *Structure and Bonding in Crystals*; O'Keeffe, M., Navrotsky, A., Eds.; Academic Press: New York, 1981; Vol. 2, pp 1−30.
(24) Müller, A.; Kögerler, P.; Kuhlmann, C. A variety of combinatory linkable units as disposition: from a giant icosahedral Keplerate to multi-functional metal-oxide based network structures. *Chem. Commun.* **1999**, *15*, 1347−1358.
(25) Liu, T. Hydrophilic Macroions Solutions: What Happens when soluble ions reach the size of nanometer scale? *Langmuir* **2010**, *26*, 9202−9213.
(26) Liu, T.; Diemann, E.; Li, H.; Dress, A. W.; Müller, A. Self-assembly in aqueous solution of wheel-shaped Mo_{154} oxide clusters into vesicles. *Nature* **2003**, *426*, 59.
(27) Liu, T.; Imber, B.; Diemann, E.; Liu, G.; Cokleski, K.; Li, H.; Chen, Z.; Müller, A. Deprotonations and charges of well-defined $\{Mo_{72}Fe_{30}\}$ nanoacids simply stepwise tuned by pH allow control/variation of related self-assembly processes. *J. Am. Chem. Soc.* **2006**, *128*, 15914−15920.
(28) Zhang, J.; Li, D.; Liu, G.; Glover, K. J.; Liu, T. Lag periods during the self-assembly of $\{Mo_{72}Fe_{30}\}$ macroions: connection to the virus capsid formation process. *J. Am. Chem. Soc.* **2009**, *131*, 15152−15159.
(29) Hiemenz, P. C. *Principles of Colloid and Surface Chemistry*; M. Dekker: New York, 1986; Vol. *188*.
(30) Woodruff, D. N.; Winpenny, R. E. P.; Layfield, A. R. Lanthanide single-molecule magnets. *Chem. Rev.* **2013**, *113* (7), 5110−5148.
(31) Davranche, M.; Gruau, G.; Dia, A.; Le Coz-Bouhnik, M.; Marsac, R. *Rare Earth Elements in Wetlands*; Taylor & Francis Group/CRC Press: New York, 2017; pp 135−162.
(32) Wheelwright, E. J.; Spedding, F. H. The use of chelating agents in the separation of the rare earth elements by ion-exchange methods. Ames Laboratory ISC Technical Reports; Ames Laboratory, 1955.
(33) Quinn, J. E.; Soldenhoff, K. H.; Stevens, G. W.; Lengkeek, N. A. Solvent extraction of rare earth elements using phosphonic/phosphosnic acid mixtures. *Hydrometallurgy* **2015**, *157*, 298−305.
(34) Yin, X.; Wang, Y.; Bai, X.; Wang, Y.; Chen, L.; Xiao, C.; Diwu, J.; Du, S.; Chai, Z.; Albrecht-Schmitt, T. E.; Wang, S. Rare earth separations by selective borate crystallization. *Nat. Commun.* **2017**, *8*, 14438.

https://dx.doi.org/10.1021/jacs.0c07146
J. Am. Chem. Soc. 2020, 142, 17508−17514